LA-UR -84-1314
CONF-841059--1

LA-UR--84-1314

DE84 011418

Los Alamos National Laboratory is operated by the University of California for the United States Department of Energy under contract W-7405 ENG-36

TITLE: Towing Tank Studies of Stratified Flow over Ridges and Valleys

AUTHOR(S): J. T. Lee and Sumner Barr (Los Alamos National Laboratory, ESS-7, MS D466, Los Alamos, NM 87545)

Robert E. Lawson, Jr., and William H. Snyder (U.S. Environmental Protection Agency, Research Triangle Park, NC 27709)

G. L. Marsh (Northrop Services, Inc., Research Triangle Park, NC 27711)

SUBMITTED TO: American Meteorological Society Third Conference on Mountain Meteorology, Oct. 15-19, 1984, Portland, OR

DISCLAIMER

This report was prepared as an account of work sponsored by an agency of the United States Government. Neither the United States Government nor any agency thereof, nor any of their employees, makes any warranty, express or implied, or assumes any legal liability or responsibility for the accuracy, completeness, or usefulness of any information, apparatus, product, or process disclosed, or represents that its use would not infringe privately owned rights. Reference herein to any specific commercial product, process, or service by trade name, trademark, manufacturer, or otherwise does not necessarily constitute or imply its endorsement, recommendation, or favoring by the United States Government or any agency thereof. The views and opinions of authors expressed herein do not necessarily state or reflect those of the United States Government or any agency thereof.

MASTER

By acceptance of this article, the publisher recognizes that the U.S. Government retains a nonexclusive, royalty-free license to publish or reproduce the published form of this contribution, or to allow others to do so, for U.S. Government purposes.
The Los Alamos National Laboratory requests that the publisher identify this article as work performed under the auspices of the U.S. Department of Energy

Los Alamos Los Alamos National Laboratory
Los Alamos, New Mexico 87545

FORM NO 836 R4
ST NO 2629 5/81

DISTRIBUTION OF THIS DOCUMENT IS UNLIMITED

TOWING TANK STUDIES OF STRATIFIED FLOW OVER RIDGES AND VALLEYS

by

J. T. Lee and Sumner Barr
Atmospheric Sciences Group
Earth and Space Sciences Division
Los Alamos National Laboratory
Los Alamos, NM 87545

Robert E. Lawson, Jr.* and William H. Snyder*
Meteorology and Assessment Division
Environmental Sciences Research Laboratory
U.S. Environmental Protection Agency
Research Triangle Park, NC 27711

and

G. L. Marsh
Northrop Services, Inc.
Research Triangle Park, NC 27709

ABSTRACT

Stable atmospheric flow over a ridge and a valley was simulated in a large towing tank filled with stratified salt water. Flow visualization experiments were conducted using colored dye streamers and 10 cm high models with sinusoidal cross-sections. These experiments provided qualitative data on the structure of the flow field over the ridges and within the valley. They also provided quantitative data on the height of the dividing streamline which separates the fluid that flows over a ridge from that which flows around the ends. These data agree with an existing theory based upon the potential energy barrier associated with flow over the ridge.

---

*On assignment from the National Oceanic and Atmospheric Administration, U.S. Dept. of Commerce.

1. INTRODUCTION

Winds near the ground are strongly influenced by the topography of the surrounding area. In particular, there is a tendency for the wind to be deflected by ridges and channeled along valleys. An understanding of these phenomena and the ability to predict the magnitude and direction of local winds is needed for analyzing atmospheric transport and dispersion in areas of complex terrain.

Local winds are also influenced by other factors such as the stratification of the atmosphere, the diurnal heating and cooling cycle, Coriolis forces, and large scale circulation patterns. A discussion of these phenomena is presented in numerous references, e.g., Orgill (1981), Atkinson (1981), and Scorer (1978). It is difficult to consider all of these effects simultaneously and make any progress toward understanding the basic physics of the flow. However, by focusing upon one aspect at a time in controlled experiments, an understanding of the importance of the various flow phenomena can be obtained. One useful approach is the testing of small-scale models in flow simulation facilities such as wind tunnels and towing tanks.

In a previous paper Lee et al. (1981) presented results from a wind tunnel study of flow channeling produced by ridges and valleys under neutral atmospheric conditions when the ambient wind is at an oblique angle to the axis. The general objective of the present study was to extend these experiments to stable flow conditions. This was accomplished by conducting flow visualization experiments in a stratified towing tank. A brief description of the facility and the models is presented below, followed by typical photographs and a discussion of the observed flow patterns about ridges and valleys.

2. EXPERIMENTAL FACILITY AND MODELS

The experiments were conducted in the large stratified towing tank at the EPA Fluid Modeling Facility in Research Triangle Park, NC. A detailed description of this facility is presented in Thompson and Snyder (1976) and Hunt, Snyder, and Lawson (1978). The tank is 1.2 m deep, 2.4 m wide, and 24 m long. It is constructed of an aluminum frame with acrylic plastic panels in the bottom and sides to permit viewing from almost any position and angle. The tank is connected to a filling system that allows the establishment of an arbitrary stable density profile using salt water with specific gravity of 1.0 to 1.2.

Models are mounted flush on a 2.4 m square baseplate. The baseplate is inverted and mounted beneath a towing carriage which runs along the full length of the top of the tank. During a tow the model is upside down and completely submerged, and the edge of the baseplate is typically 3 or 4 mm below the surface of the water. The carriage is pulled by cables which are driven by a motor mounted at the end of the channel. Towing speeds can be varied from 3 to 50 cm/s. Illumination of the model is provided by fluorescent tubes along the outer edges of the bottom of the tank and a back-light panel which is attached to the towing carriage on one side of the tank.

Details of the ridge model are shown in Fig. 1. It has a sinusoidal cross-section as given by the relation

$$z = (h/2)[1 + \cos(2\pi x/W)] \qquad (1)$$

The ridge height h is 10 cm and the width W is 37 cm which results in a maximum slope of 40^{o}. This is the same shape and dimensions as the steep ridge model used in the previous wind tunnel study, Lee et al. (1981). The length of the

straight section L is 163 cm resulting in a length-to-width ratio of 4.4. The end caps have the same sinusoidal cross-section in vertical planes with a circular cross-section in horizontal planes. The ridge was molded into a flat circular plate which fits flush into the carriage baseplate so that the wind angle θ could be changed by rotating the circular plate. When the ridge is normal to the tow direction, $\theta = 90^{\circ}$, the maximum cross-sectional area along the length of the ridge is 75% of the area defined by the product of the ridge height and the tank width. Thus the minimum flow area through the gaps at the ends of this model is 25% of the cross-sectional area of a two-dimensional ridge that extends completely across the tank. A valley model was constructed from two of these ridges placed together as shown in Fig. 2.

Linear density profiles were used for all of the experiments in this study. The nominal value of the Brunt-Vaisala frequency, $N = [-(g/\rho)(d\rho/dz)]^{1/2}$, was 1.3 s^{-1}. Between runs the density profile was checked by withdrawing samples at various depths and measuring their specific gravity with an electronic balance. The density profile after a run sometimes deviated from the linear profile that existed before the run. Linearity was restored by skimming a shallow layer of water off the surface and refilling the tank from the bottom with an equal amount of saturated salt water. Typical density profiles before a run, after a run, and after skimming and refilling are shown in Fig. 3.

3. RESULTS AND DISCUSSION

Two series of experiments were conducted with the objectives of obtaining quantitative data on the height of the dividing streamline for an isolated ridge and qualitative data on flow channeling for a ridge and a valley. Data and typical photographs from these studies are presented and discussed below.

3.1 DIVIDING STREAMLINE EXPERIMENTS FOR AN ISOLATED RIDGE

Probably the simplest and most useful concept in the analysis of stable flow over an obstacle is that of the dividing streamline. This is illustrated schematicaly in Fig. 4 where h_s is the height of the dividing streamline, sometimes called the critical height, and h is the height of the ridge. A theory for this type of flow based on the following simple energy considerations was first presented by Sheppard (1956). The kinetic energy of the flow along streamlines which originate at upstream elevations below h_s is less than the increase in potential energy that is required for the fluid to be lifted over the ridge. Therefore, these streamlines must pass around the ridge as shown by the dashed lines. The kinetic energy of the flow along streamlines which originate above h_s is greater than the required increase in potential energy. Therefore, these streamlines can pass over or around the ridge. By equating the kinetic energy of the approach flow at the dividing streamline elevation h_s to the increase in potential energy required to lift the fluid from the dividing streamline elevation to the top of the hill, Sheppard derived a general formula for h_s. For an incompressible stratified fluid his result can be expressed as

$$\rho U^2(z = h_s)/2 = -g\int_{h_s}^{h} (h-z)(d\rho/dz)dz \qquad (2)$$

where the density and velocity, ρ and U, are, in general, functions of the vertical coordinate z. This integral formula can be solved by iteration for h_s with arbitrary density and velocity distributions in the approach flow. For a linear density profile and a uniform velocity it can be reduced to the simple relation

$$h_s = h(1-F) \qquad (3)$$

where F is the Froude number, F = U/Nh. A detailed review and analysis of the theoretical and experimental basis for the dividing streamline concept, including part of the data from this study, is presented by Snyder et al. (1982). These authors also point out some of the theoretical inconsistencies associated with the simple energy arguments presented above.

The flow pattern in Fig. 4 will exist for a simple ridge of any finite length under very stable conditions. This implies that the approximation of two-dimensional flow in vertical planes is not appropriate for finite length ridges even if they are very long. The flow around the ridge below the dividing streamline provides a mechanism by which plumes can be diverted large distances away from trajectories based on the ambient wind. Of course real ridges frequently have gaps through which plumes can pass. A plume can also impinge on the ridge resulting in local areas of high concentration.

All of the experiments were conducted with a carefully maintained linear density profile similar to those in Fig. 3. The Froude number F was varied from 0.3 to 1.0 by varying the tow velocity U from 4 to 13 cm/sec. Wind angles θ of 90°, 60°, and 30° were used. In most of the experiments two streamers of dye, one red and one blue, were released from a vertical stack consisting of two small tubes attached to the center of the leading edge of the baseplate. The ends of the tubes were bent 90° so that the dye was injected toward the model and parallel to the flow. The flow rate of the dye was adjusted to provide a nearly isokinetic release. Neutral density of the dye streamers was assured by mixing the dye with water drawn just before an experiment from the level in the tank at which the dye was injected during the experiment. The vertical separation between the ends of the two tubes was 2 cm with the red dye

released above* the blue dye. The height of the stack was then varied for each experiment until a position was found such that the red dye passed over the ridge and the blue dye was blocked and diverted around the ends of the ridge. Under these conditions the dividing streamline can be regarded as being midway between the two release points with a maximum error of ±1 cm. Since the dye streamers have a finite width of approximately 1 cm when they reach the model, a more realistic estimate of the error is probably ±0.5 cm which is ±5% of the ridge height. The flow fields were photographed from the side using movie, video and 35 mm cameras attached to the tow carriage and from below using a hand-held 35 mm camera.

A typical series of photographs of the ridge model normal to the flow is presented in Fig. 5 for Froude numbers of 0.3 and 0.5 and theoretical values of h_s of 7 and 5 cm, respectively. The red and blue dye was released along the centerline of the model at heights that were, respectively, 1 cm above and 1 cm below the theoretical value of h_s. The photographs were taken at distances x of 5, 10, and 15 m downstream of the initial position of the model. In general the red dye passed over the ridge and the blue dye was blocked. The blue dye accumulated ahead of the ridge and flowed around either the left or right end with no obvious preference. This flow pattern switched from end to end once or twice during a tow.

For the case with a Froude number of 0.3, both the red and blue dye passed over the ridge near the end of the tow as shown in Fig. 5-c. This suggests that the effective Froude number of the approach flow becomes larger toward the

---

*The red dye was actually below the blue dye in the tank. However, the experimental procedures and results are discussed throughout this report as though the model was in the normal upright position as opposed to the inverted position that was used during the experiments. The ambient flow is from left to right in all of the photographs.

end of the tow. This has been explained by Snyder et al. (1982) as being caused by the squashing phenomenon in which the accumulation of blocked fluid ahead of the model reduces the density gradient in a layer whose depth is the same order as the height of the model. It appears that this phenomenon is associated with the finite width of the tank and could be eliminated by increasing the area of the gaps between the ends of the model and the side walls of the tank. It has no counterpart for real finite-length ridges in the atmosphere where the flow around the ends of the ridge is not restricted by the presence of walls.

The importance of the side walls is further illustrated by the photographs in Fig. 6. Conditions for this experiment were the same as in Fig. 5d-f, but the gaps between the ends of the model and the side walls of the tank were blocked with styrofoam inserts. The inserts were the same height as the ridge and fit closely against the model and the side walls so that no flow could pass around the ends of the model. The Froude number was 0.5 and the red and blue dye was released at heights of 6 cm and 4 cm respectively, i.e. 1 cm above and 1 cm below h_s. Both of these dye streamers flowed over the model during the entire tow. The green dye was released at a height of 2 cm and was turned on about midway through the tow. Part of this dye flowed over the ridge, but it also accumulated in the blocked flow region ahead of the model and appeared to be unsteady during the entire run. As pointed out by Snyder et al. (1982), it seems unlikely that the flow field for this two-dimensional ridge reaches a steady state during the tow. Results obtained with models of this type for low Froude numbers, $F < 1$, are of questionable applicability to stratified flow over finite-length ridges in the atmosphere.

Observed flow patterns for dye released along the centerline of the ridge with a wind angle of $\theta = 60^{o}$ were similar to those with $\theta = 90^{o}$. However, the dye released below the dividing streamline flowed around the downstream end of the model during the entire tow instead of switching from end to end. With $\theta = 30^{o}$ there were some significant differences. Typical photographs for $\theta = 30^{o}$ and $F = 0.5$ are presented in Fig. 7. In Fig. 7-a the red and blue dye was released at heights of 6 and 4 cm respectively. Both of these streamers go around the downwind end of the model. In Fig. 7-b the red and blue dye release points were raised to 8 and 6 cm respectively, and the red dye flowed over the ridge. Thus the dividing streamline was located at a height of 7 ± 1 cm compared to the theoretical value of $h_s = 5$ cm. However, this does not violate the dividing streamline concept which states that flow originating upstream above the theoretical value of h_s has enough kinetic energy to flow over the ridge but is not constrained to do so.

Top views from experiments in which dye was released at three different lateral positions with $\theta = 30^{o}$ and $F = 0.5$ are shown in Fig. 8. The lateral spacing between the release points was 17.5 cm with one of the streamers released on the centerline of the model. In Fig. 8-a and 8-b, the release height was 4 cm, and all of the dye streamers flowed around the model as would be expected. Figures 8-a and 8-b were taken at different positions along the tank during the same tow. Figure 8-a shows that the center streamer impinged on the model at the stagnation point. This flow pattern was not steady, however, as shown in Fig. 8-b where the center streamer flowed downwind of the stagnation point. In Fig. 8-c the three dye streamers were released at $z = 6$ cm, and only the center one flowed over the model. Thus, near the stagnation point, the height of the dividing streamline is approximately 5 cm in agreement with the theory. These experiments show that the lateral position of the

source relative to the stagnation point has an effect on whether a plume goes over, around, or impinges on a ridge.

Quantitative data from the dividing streamline experiments with dye released along the centerline of the model are summarized in Figs. 9, 10, and 11 for $\theta = 90^{o}$, 60^{o}, and 30^{o} respectively. Open symbols indicate that the dye flowed over the top of the model, closed symbols that the dye was blocked by the model and flowed around the ends, and half closed symbols that the dye impinged near the top of the model with part of the dye flowing over the top and part of it being blocked. The data for $\theta = 90^{o}$ and 60^{o} are consistent with the theoretical relation $h_s/h = (1 - F)$. The data for $\theta = 30^{o}$ are better described by the relation $h_s/h = (1 - 0.7F)$. However, as discussed above, these data are applicable to the centerline of the ridge. Significant departures from these results can be expected for different lateral positions if the wind angle is small.

3.2 FLOW CHANNELING EXPERIMENTS FOR RIDGES AND VALLEYS

Wind tunnel studies of flow channeling in valleys were conducted by Lee et al. (1981). The emphasis in that study was on the effects of the aerodynamic interaction of the flow with the ridges that form the valley when the wind is at an oblique angle to the axis. Two general types of valleys were tested: a steep valley with flow separation on the lee side of the ridges and a gentle valley with no flow separation. The channeling of the flow was much greater within the steep valley. This channeling was not the result of physical confinement by the two ridges of the valley, however, since similiar flows were observed downwind of a single steep ridge. This flow pattern was explained qualitatively by the superposition of the component of the ambient flow parallel to the ridge with the recirculating flow in the separated region downstream of the ridge to produce a spiraling flow along the axis.

Separated flows of the type observed in the steep valley produce a high level of turbulent mixing between the flow in the separated region and the ambient flow. Therefore, material released in the valley will be entrained into the ambient flow and will not be transported long distances along the valley. Experiments by Bell and Thompson (1980) have shown that stable stratification prevents this ventilation of the valley by turbulent mixing with the ambient flow. Therefore, it seems likely that transport along the valley will be increased under stable atmospheric conditions.

The objective of this part of the present study was to extend the wind tunnel experiments to stable flow conditions. Experiments were conducted in the towing tank with the ridge model at wind angles θ of 90^{o} and 60^{o} and the valley model at 60^{o}. Linear density profiles with $N \approx 1.3\ s^{-1}$ were used. Since these experiments were intended to produce qualitative results, the linearity was not controlled as carefully from run to run as in the dividing streamline experiments. For each experiment the desired value of the critical height h_s was selected before the run. The required tow velocity was obtained by solving Eq. 2 for U using the measured density profile. The effective Froude number for the run was then obtained by solving Eq. 3 for F. Experiments were conducted over a Froude number range of 0.3 to 1.7 with tow velocities of approximately 3 to 24 cm/sec. Dye streamers were released at various positions ahead of the model and through the baseplate. Photographs were taken with tripod-mounted and hand-held 35 mm cameras from the side, a tripod-mounted 35 mm camera from below, and a 16 mm movie camera at a fixed side position.

Figures 12 and 13 show side and top views of the streamline patterns over the ridge and valley models respectively with a wind angle θ of 60^{o} and a Froude number range of 0.3 to 1.7. In these experiments eleven neutral density

dye streamers were released from a rake of tubes suspended from the leading edge of the baseplate. Each tube was bent 90° toward the model and the dye was injected at a nearly isokinetic rate parallel to the ambient flow. The lowest release point was 2 cm above the base plate (0.2 h) and, with a spacing of 2 cm between tubes, the highest release point was at a height of 22 cm (2.2 h).

The general nature of stratified flow over a ridge is discussed by Hunt et al. (1978). For ridges with rounded crests and moderate slopes, the character of the flow depends primarily on the ratio of the wavelength of the lee waves, $\lambda = 2\pi U/N$, to the width of the ridge, W. This ratio can be written as $\lambda/W = 2\pi(h/W)F$ and, for the ridge used in this study, $\lambda/W = 1.7\ F$. For $\lambda >> W$ ($F >> 1$) the flow over the ridge is essentially the same as for neutral conditions and separation on the lee slope of the ridge is controlled by the flow in the boundary layer. This is illustrated by the streamline patterns in Fig. 12-a. The formation and influence of the lee waves when $\lambda/w = 1.5$ are apparent in Fig. 12-b where separation occurs further down the lee slope and another separated flow region or rotor appears under the crest of the lee wave. For $\lambda < W$ ($F < 0.6$), separation is controlled by the pressure distribution produced by the lee waves. This is illustrated in Figs. 12-c and 12-d where separation on the lee slope is eliminated for $F = 0.5$ and 0.3. Under these conditions the strong rotor located immediately downwind of the ridge dominates the flow field.

The streamline patterns over the valley model, Fig. 13, are similar to those over the ridge. Separation from the lee side of the second ridge is eliminated for $F = 0.5$ and 0.3, and a strong rotor is formed downstream of the second ridge. Flow separation on the lee side of the first ridge was not eliminated at any value of F. This separation appeared to be controlled by the boundary layer and produced a separated region in the valley for all values of

F. It appears that the two ridges are close enough together to act as a single ridge as far as the general flow pattern over the model and the lee wave pattern are concerned.

The top views in Figs. 12 and 13 show that the streamlines which pass over the model are deflected slightly in the crosswind direction toward the upstream end of the model. This was also observed in the wind tunnel experiments, Lee et al. (1981), and was explained by the acceleration of the component of the ambient flow that is normal to the ridge as it flows over the model. A large part of the dye is deflected around the downwind ends of the models for F = 0.3. Analysis of these photographs show that they are consistent with the theoretical relation for the dividing streamline height h_s as given by Eq. 2.

There is no evidence in Fig. 13 of dye flowing along the valley. This is misleading, however, and results from the rapid dilution of any dye that is entrained into the separated flow in the valley. To better illustrate this entrainment a large dye streamer was released from the leading edge of the baseplate. These photographs are shown in Fig. 14 for F = 0.5. In Fig. 14-a the dye was released very near the theoretical critical height h_s. Most of this dye passed over the first ridge and was trapped in the valley. It then flowed along the valley and out the downstream end. In Fig. 14-b the dye was released slightly above the critical height. It cleared both ridges of the valley and flowed into the rotor downstream of the second ridge. Thus the amount of dye which is entrained into the valley depends very strongly on the release height relative to the critical height h_s.

The channeling of plumes in the separated region downstream of a ridge is illustrated in Figs. 15 and 16. Figure 15 shows a large neutrally buoyant dye streamer injected through the baseplate at the downstream edge of the ridge. For F = 1.7, Fig. 15-a, the dye spirals downwind along the lee side of the

ridge as in the wind tunnel experiments, Lee et al. (1981). This is essentially a neutral flow condition as can be seen by comparison to Fig. 15-e which was taken under neutral conditions at the same velocity. The turbulence in the separated zone produces rapid mixing of the dye. As the Froude number is decreased, the turbulent mixing is reduced. At F = 0.5, Fig. 15-c, the dye is swept up by the rotor and flows downwind essentially parallel to the ambient flow. At F = 0.3 the flow changes drastically as shown in Fig. 15-d. Here the turbulent mixing seems to be completely suppressed and the dye puddles along the base of the model in both the upwind and downwind directions. A similar series of experiments with the valley model is shown in Fig. 16-a through 16-d where the dye was released at the center of the valley floor. These experiments also showed a reduction in turbulent mixing between the ambient flow and the flow within the valley as the Froude number was decreased. This effect is illustrated more clearly in the movies of the experiments than in these still photographs. These qualitative results are consistent with the more precise quantitative experiments of Bell and Thompson (1980) which show that ventilation of a valley is suppressed for Froude numbers less than 1.3.

The effect of Froude number on the flow in the separated region is complicated by Reynolds number effects. Since the Froude number is decreased by decreasing the tow velocity, the Reynolds number also decreases. The Reynolds number based on the height of the hill, h = 10 cm, varies from approximately 23,000 to 4,000 as F changes from 1.7 to 0.3. Based on the fetch from the leading edge of the baseplate to the center of the model the corresponding Reynolds number variation is 300,000 to 52,000. The Reynolds numbers for the lower Froude numbers are low enough to suggest the possibility of a Reynolds number effect. This interpretation is supported by Fig. 16-e which was taken under neutral conditions with a velocity and Reynolds number

equal to the value used in the F = 0.3 experiment, Fig. 16-d. At this low Reynolds number the dye puddles in the valley for both neutral and very stable conditions. The drastic change in the flow for a small change in Froude number and Reynolds number illustrated in Figs. 16-c and d suggests a laminar to turbulent transition phenomenon with laminar flow in the valley in Fig. 16-d. Thus there is definitely a Reynolds number effect at low Froude numbers in the experiments illustrated in Figs. 15 and 16, and their applicability to high Reynolds number atmospheric flows is questionable.

4. CONCLUSIONS

These experiments support the dividing streamline concept for stable flow about ridges and the use of Sheppard's (1956) integral formula for calculating the height h_s of the dividing streamline. Data obtained with our sinusoidal ridge for wind angles of 90° and 60° are in agreement with this relation. Data for a wind angle of 30° are also in agreement if the relation is interpreted as a necessary but not sufficient condition. By this we mean that the flow along streamlines that originate below h_s pass around the ridge, but flow along streamlines that originate above h_s pass over or around the ridge depending upon other factors such as the wind angle and the lateral position of the streamline relative to the stagnation point.

A second set of experiments revealed some of the qualitative features of flow channeling produced by ridges and valleys under stable conditions. These experiments suggest that increasing stability or decreasing Froude number has an effect on the transport of material along a valley due to the reduced turbulent mixing between the flow in the valley and the ambient flow. This conclusion is tentative, however, since the low Froude numbers were achieved by using low velocities and, therefore, low Reynolds numbers. The experiments

indicate that Reynolds number effects are not negligible for this type of flow under these conditions.

ACKNOWLEDGEMENTS

The participation of Los Alamos personnel in this project was supported by the U.S. Air Force and the U.S. Dept. of Energy. We gratefully acknowledge the useful suggestions and assistance of Roger S. Thompson, EPA, and William E. Clements and Gregory L. Stone, Los Alamos National Laboratory.

REFERENCES

Atkinson, B. W., 1981, Meso-scale Atmospheric Circulations, Academic Press, London.

Bell R. C. and R. O. R. Y. Thompson, 1980, "Valley Ventilation by Cross Winds, J. Fluid Mech., 96, part 4, p. 757-767.

Hunt, J. C. R., W. H. Snyder, and R. E. Lawson, Jr., 1978, "Flow Structure and Turbulent Diffusion Around a Three-Dimensional Hill: Fluid Modeling Study on Effects of Stratification, Part 1. Flow Structure," U.S. Environmental Protection Agency, EPA-600/4-78-041, Research Triangle Park, NC.

Lee, J. T., S. Barr, W. H. Snyder, and R. E. Lawson, Jr., 1981, "Wind Tunnel Studies of Flow Channeling in Valleys," Second Conference on Mountain Meteorology, American Meteorological Society, Boston, M .

Orgill, M. M., 1981, "Atmospheric Studies in Complex Terrain: A Planning Guide for Future Studies," Pacific Northwest Laboratory, PNL-3656, ASCOT 80-4.

Scorer, R. S., 1978, Environmental Aerodynamics, John Wiley and Sons, New York.

Sheppard, P. A., 1956, "Airflow Over Mountains," Quart. J. Roy. Meteor. Soc., 82, p. 528-29.

Snyder, W. H., R. S. Thompson, R. E. Eskridge, R. E. Lawson, Jr., I. P. Castro, J. T. Lee, J. C. R. Hunt, and Y. Ogawa, 1982, "The Structure of Strongly Stratified Flow Over Hills: Dividing Streamline Concept," U.S. Environmental Protection Agency, EPA-600/3-83-015, Research Triangle Park, NC (submitted to Jour. of Fluid Mech.).

Thompson, R. S. and W. H. Snyder, 1976, "EPA Fluid Modeling Facility," Proceedings of Conference on Environmental Modeling and Simulation, U.S. Environmental Protection Agency, EPA-600/9-76-016, Washington, DC.

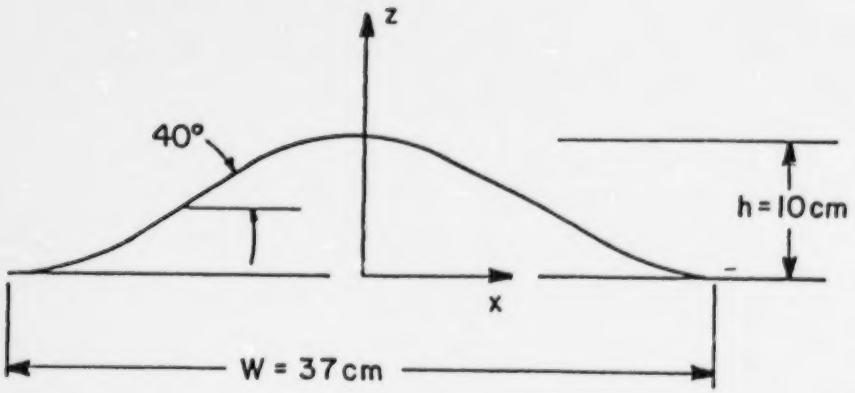

(A) CROSS - SECTIONAL VIEW

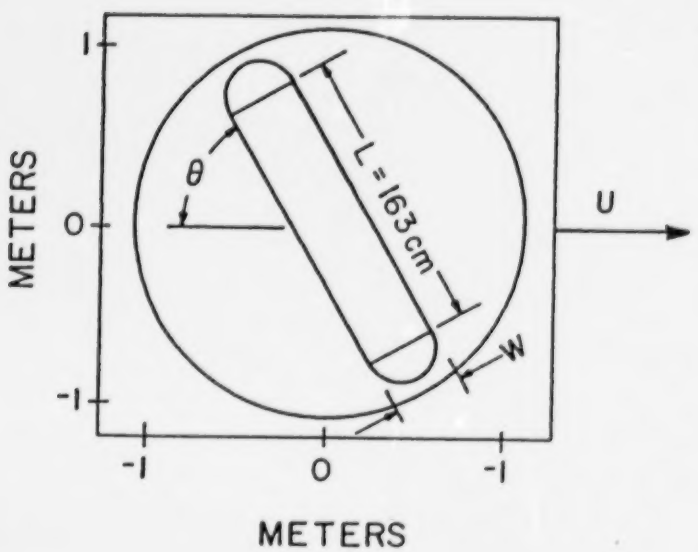

(B) PLAN VIEW OF MODEL ON BASEPLATE

Fig. 1. Details of ridge model.

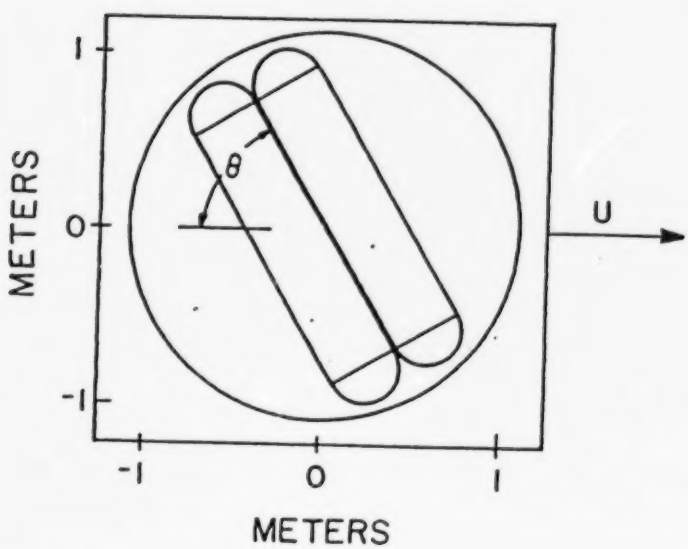

Fig. 2. Plan view of valley model on baseplate.

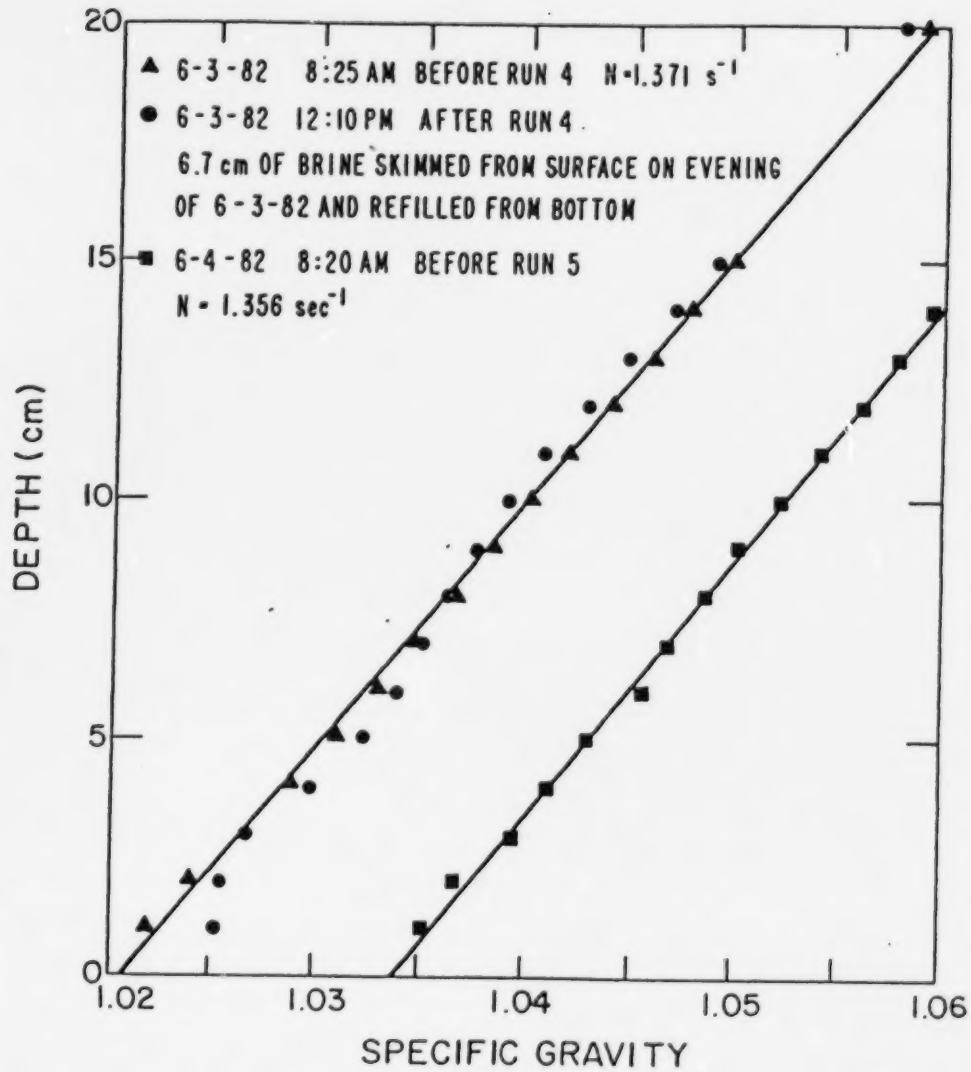

Fig. 3. Typical density profiles.

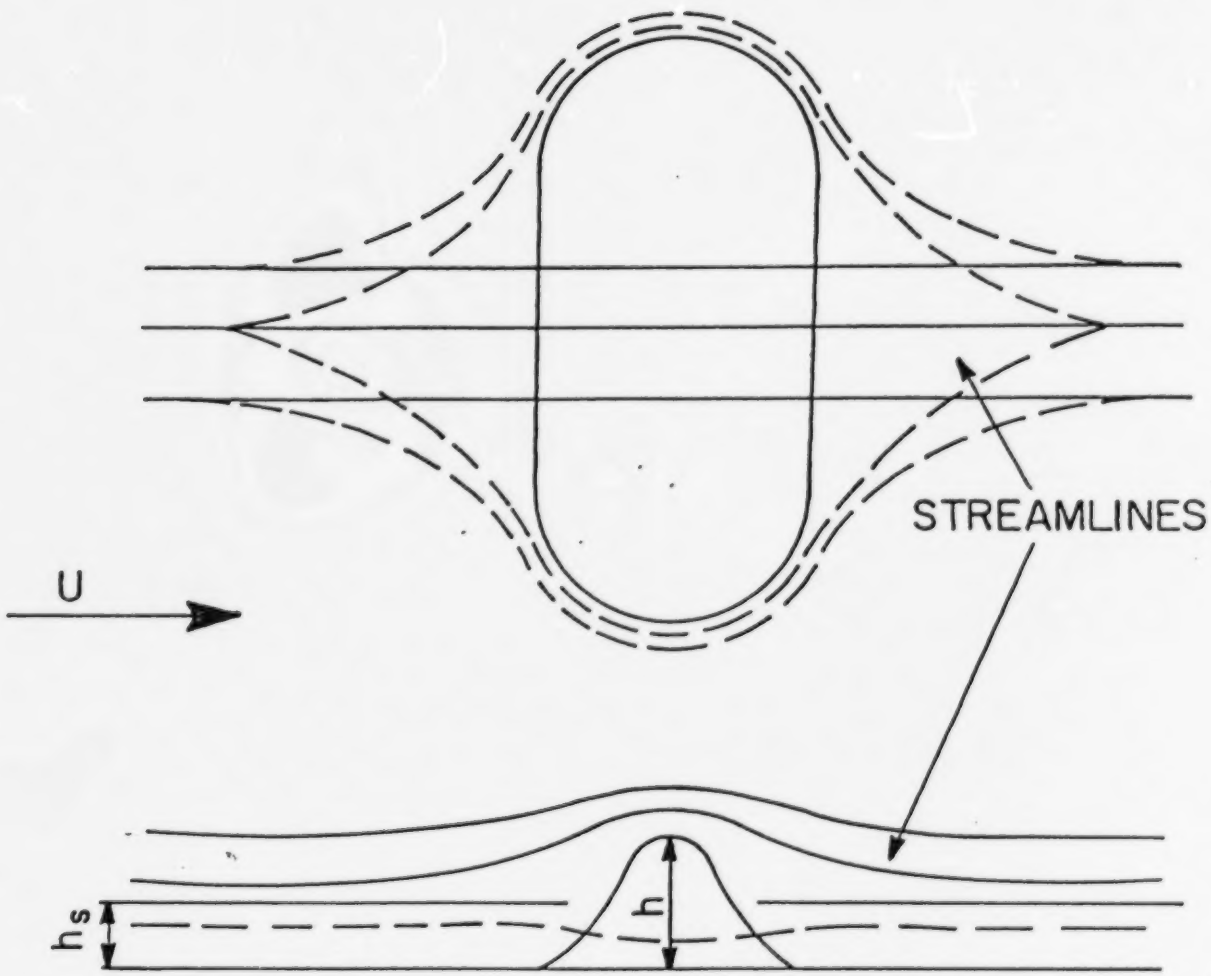

Fig. 4. Schematic of stratified flow about a ridge illustrating the dividing streamline concept.

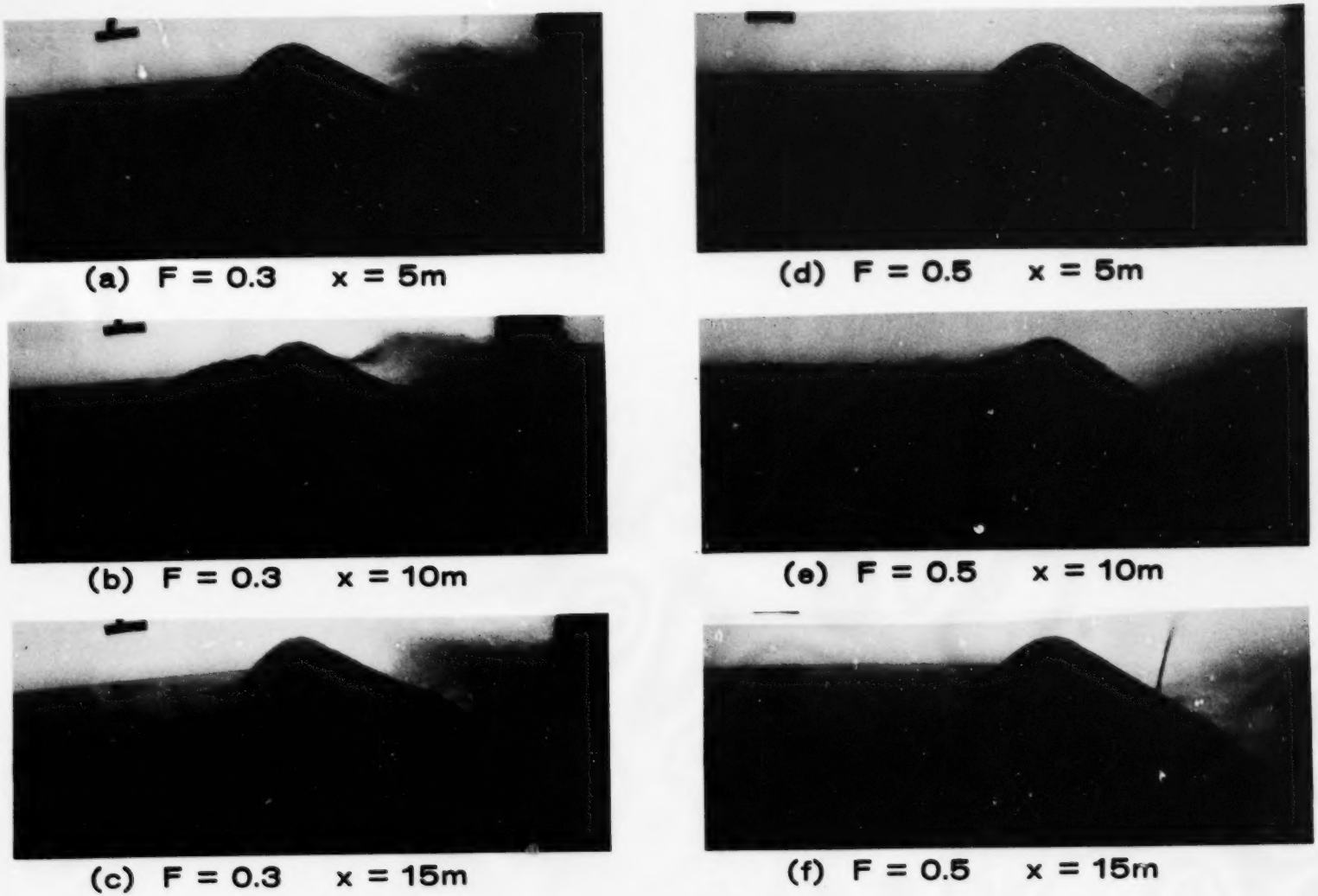

(a) F = 0.3 x = 5m

(d) F = 0.5 x = 5m

(b) F = 0.3 x = 10m

(e) F = 0.5 x = 10m

(c) F = 0.3 x = 15m

(f) F = 0.5 x = 15m

Fig. 5. Dividing streamline experiments with ridge normal to the flow, $\theta = 90°$, $h_{red} = h_s + 1cm$, $h_{blue} = h_s - 1cm$.

(a) F = 0.5 x = 5m

(b) F = 0.5 x = 10m

(c) F = 0.5 x = 15m

Fig. 6. Dividing streamline experiments for ridge with ends blocked, $\theta = 90°$, F = 0.5, h_{red} = 6cm, h_{blue} = 4cm, h_{green} = 2cm.

Top View

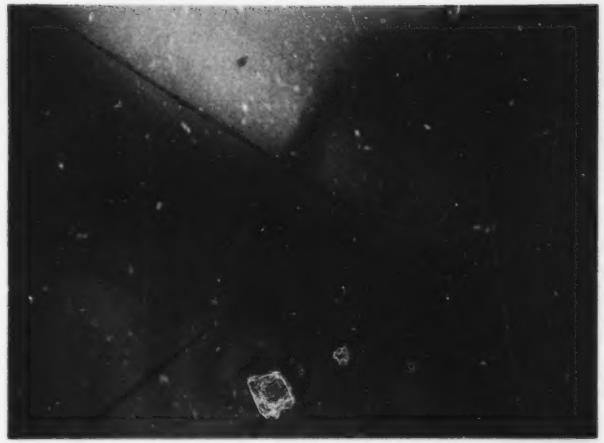

Top View

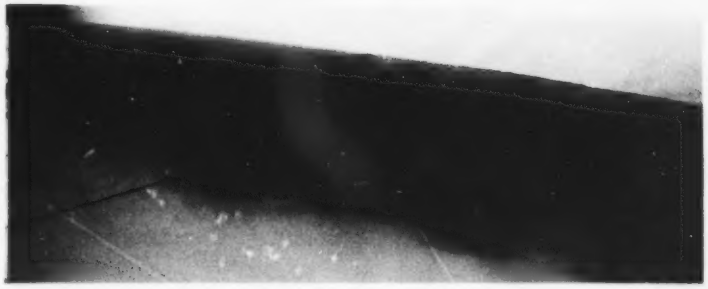

Side View

(a) h_{red} = 6cm, h_{blue} = 4cm

Side View

(b) h_{red} = 8cm, h_{blue} = 6cm

Fig. 7. Dividing streamline experiments with ridge at a wind angle of θ = 30° and F = 0.5.

(a) h_{dye} = 4cm

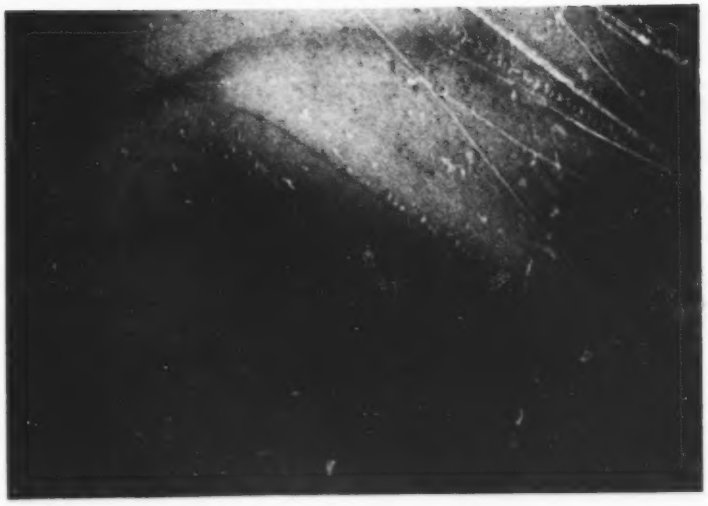

(b) h_{dye} = 4cm

(c) h_{dye} = 6cm

Fig. 8. Laterai dye release with ridge at θ = 30° and F = 0.5.

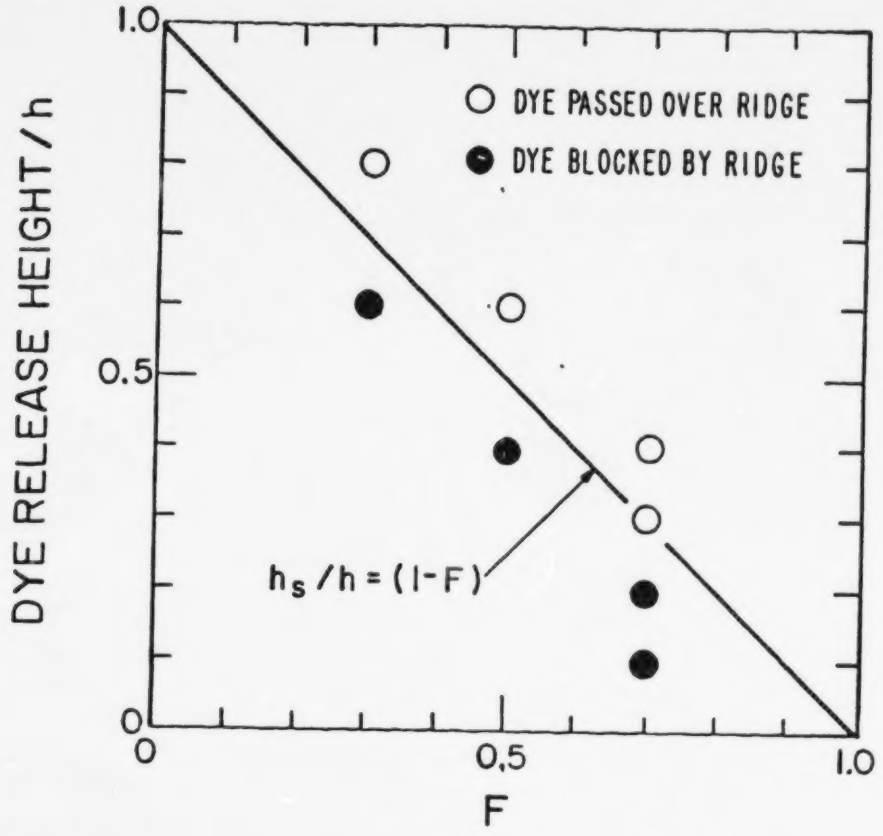

Fig. 9. Data from dividing streamline experiments for ridge normal to the flow, $\Theta = 90°$.

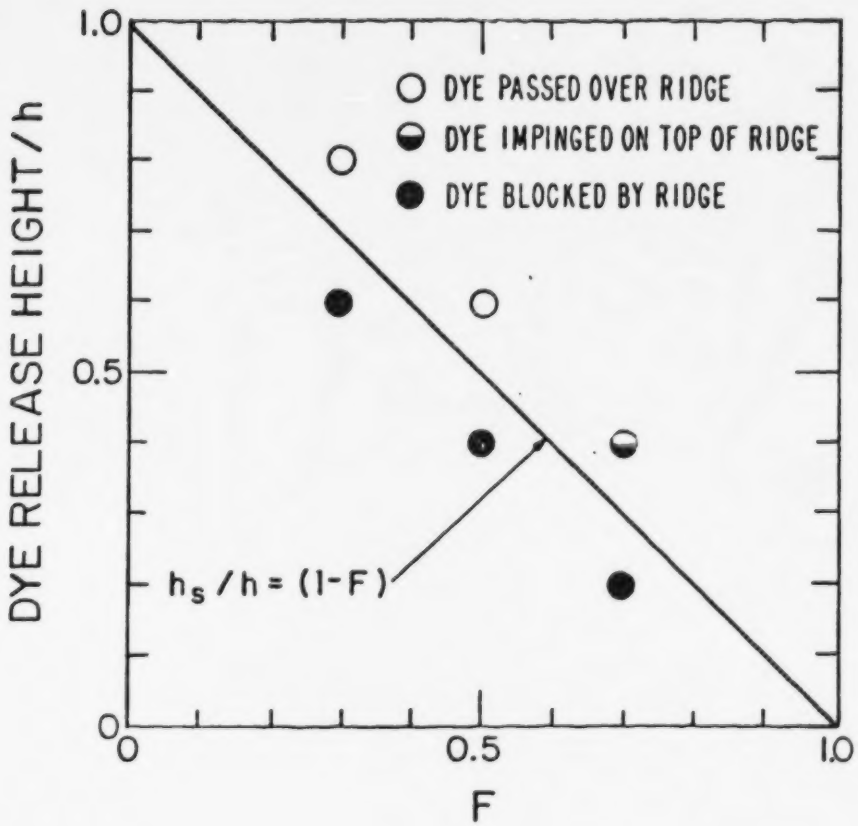

Fig. 10. Data from dividing streamline experiments for ridge with $\Theta = 60°$.

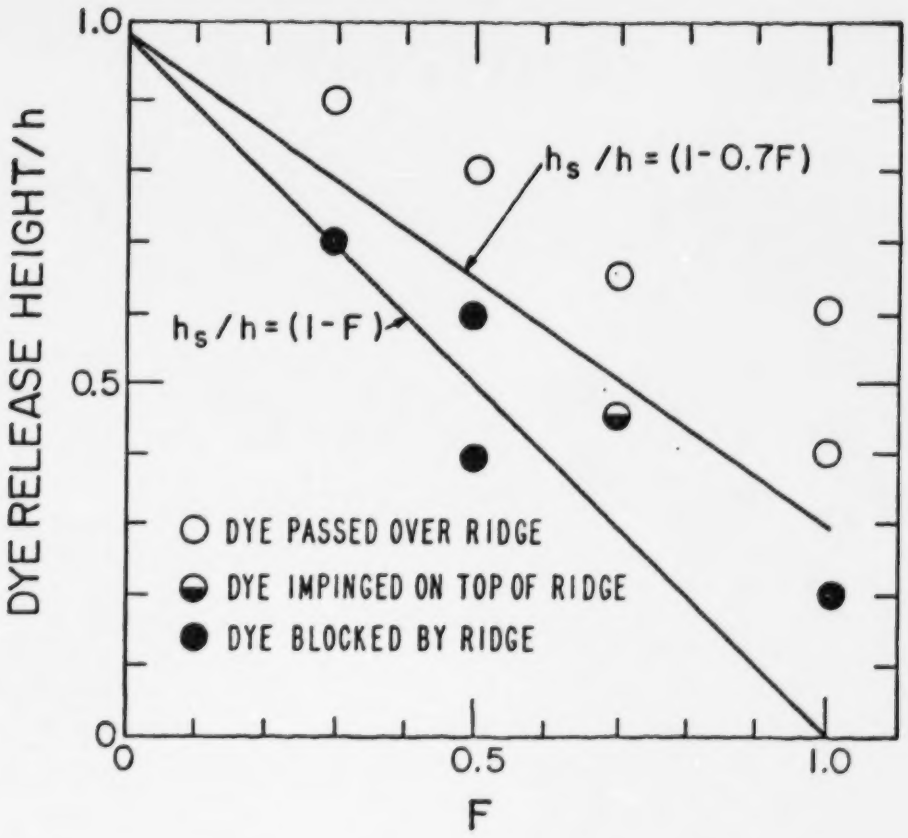

Fig. 11. Data from dividing streamline expeiments for ridge with $\theta = 30°$.

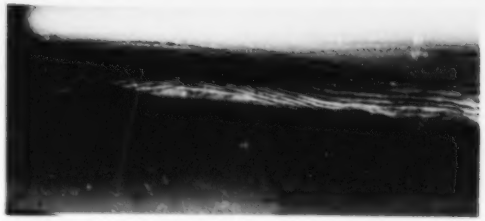

(a) F = 1.7

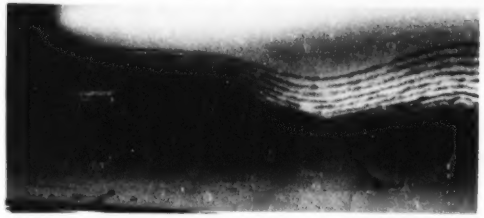

(b) F = 0.9

(c) F = 0.5

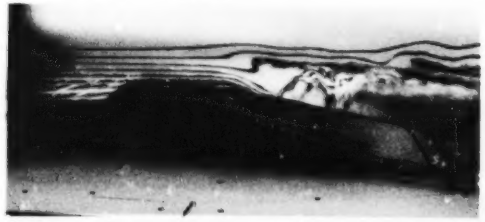

(d) F = 0.3

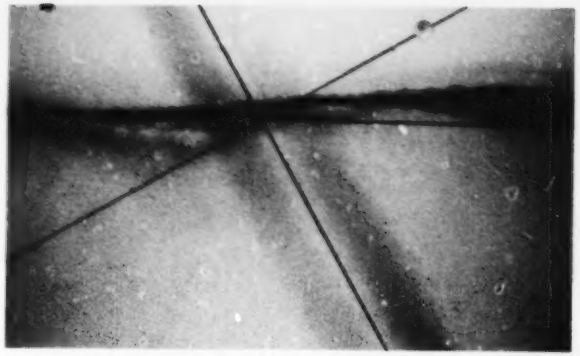

(e) F = 0.9

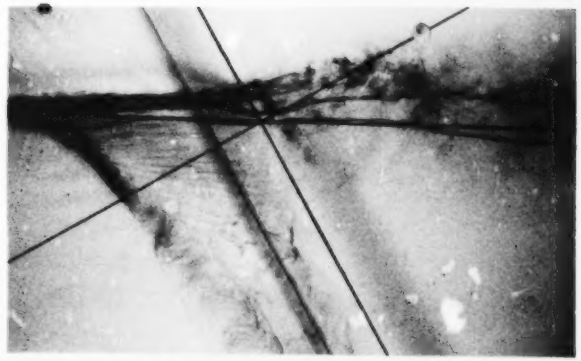

(f) F = 0.3

Fig. 12. Streamline pattern over center of ridge with a wind angle of $\theta = 60°$.

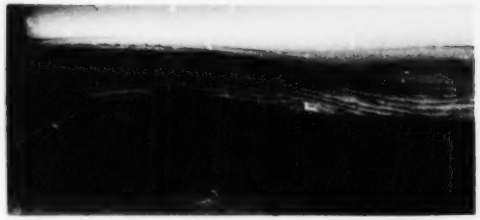

(a) F = 1.7

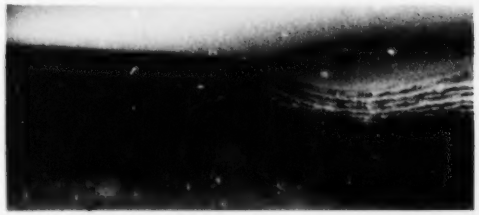

(b) F = 0.9

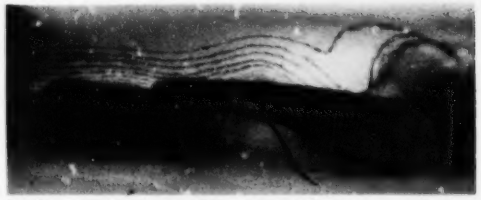

(c) F = 0.5

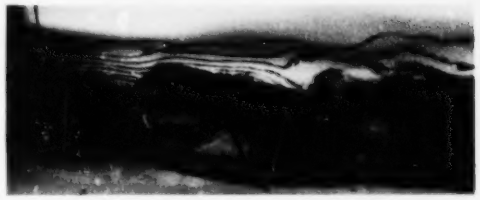

(d) F = 0.3

(e) F = 0.9

(f) F = 0.3

Fig. 13. Streamline pattern over center of valley with a wind angle of $\theta = 60°$.

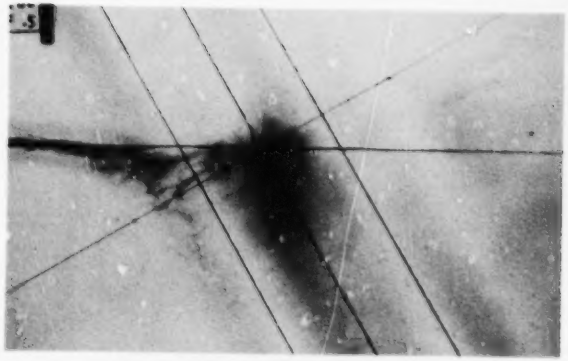

Top View

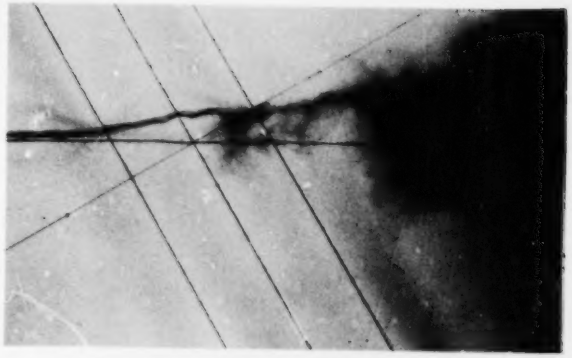

Top View

Side View

Side View

(a) $h_{dye} \approx h_s$

(b) $h_{dye} > h_s$

Fig. 14. Dye released near the critical height upstream of the valley with $\theta = 60°$ and $F = 0.5$.

(a) F = 1.7

(c) F = 0.5

(b) F = 0.9

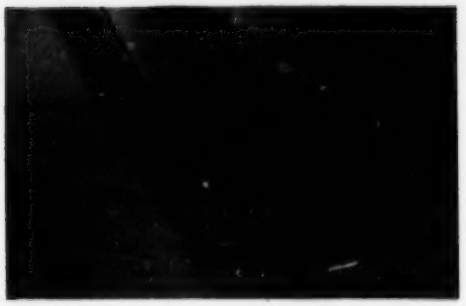

(d) F = 0.3

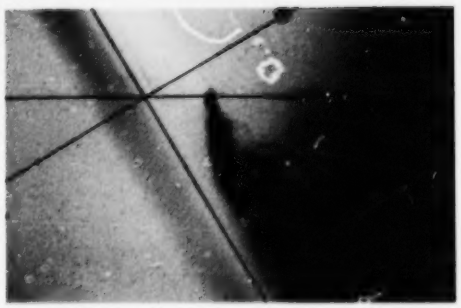

(e) $F = \infty$, $U = U_{F = 1.7}$

Fig. 15. Dye released at the downstream edge of the ridge with $\theta = 60°$.

(a) F = 1.7

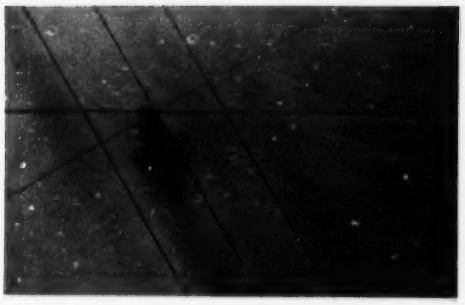

(c) F = 0.5

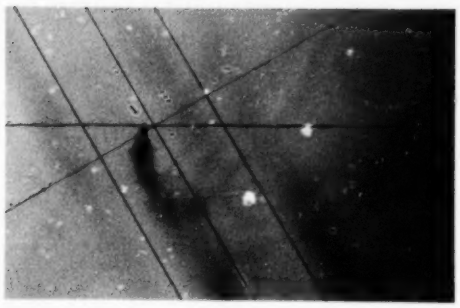

(b) F = 0.9

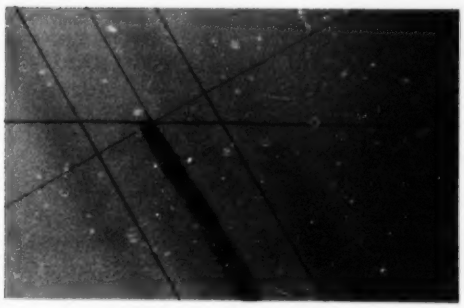

(d) F = 0.3

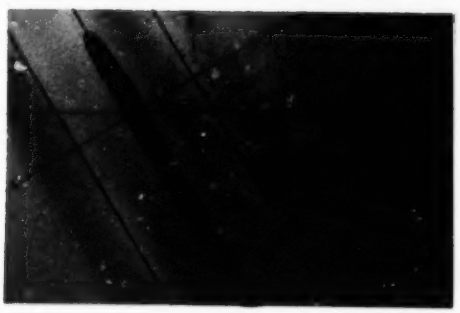

(e) $F = \infty$, $U = U_F = 0.3$

Fig. 16. Dye released at the center of the valley floor with $\theta = 60°$.